Spatial EEG Patterns, Non-linear Dynamics and Perception: the Neo-Sherringtonian View. *Brain Research Reviews 10:147-175. Freeman WJ, Skarda C (1985)*

Walter J. Freeman Journal Article e–Reprint

Spatial EEG Patterns, Non–linear Dynamics and Perception:

the Neo–Sherringtonian View

WALTER J. FREEMAN & CHRISTINE A. SKARDA

Brain Research Reviews, 10 (1985) 147–175, Elsevier, (Accepted August 27th, 1985)

Key words: brain theory – electroencephalogram (EEG) (spatial form), non–linear dynamics of EEG – olfactory perception, perception – self–organization (EEG studies) – spatial analysis of EEG

CONTENTS

1. INTRODUCTION

Recent developments in electronics have given access to new dimensions in the study of brain activity. Arrays of preamplifiers make it possible to record simultaneously from large numbers of electrodes or optical sensors placed on or in the brain, computers enable reduction and display of the immense quantities of data that rapidly accrue, and they provide the tools for constructing and testing heuristic dynamic models of brain systems. As with any new technology such as electrocardiography, X–ray imaging, electron microscopy, tomography and so forth, several years of experimentation are

required to explore its possibilities, the kinds of patterns it reveals, and what they might mean. Large series of images are necessary to give observers a sense of familiarity and confidence in what they see or do not see. New subsidiary techniques are needed for electrode design and manufacture, for preparation of animals to give access to recordings, and for data collection and processing. Standardized experiments are required to serve as benchmarks, and rules of evidence or criteria for the validity of data must be formulated. An appropriate nomenclature and convenient set of conventions for graphic display must be agreed upon.

Most importantly, a body of theory must be developed as the basis for correct processing, display, evaluation and interpretation of these new data. Present technology has already let loose a flood of new data and provided sophisticated devices for 2–D display of various facets, but the major problem is to develop some expectations of what the data should reveal. The situation is analogous to that of archeologists faced with an undeciphered written language; only by deducing some underlying rules from the specimens and their functional context can they distinguish meaningful form from adventitious artifact, or 'signal' from 'noise'. For neurophysiologists this means that a curve or a surface, which is the prediction of a model such as the solution of a set of equations, must be fitted to the processed data. The specification is: 'This is what the data ought to look like, if what we believe is valid.' If the agreement is poor, either the belief is changed or the data are processed in a different way. Although non–scientists commonly suppose that disagreement is cause for rejection of a theory, the usual outcome in good science is disclosure of an artifact or deficit in data processing.

This essay contains a review of procedures for collecting and processing multiple electroencephalograms (EEGs) from the olfactory bulb and cortex of the cat and rabbit[35], some examples of the data, some theoretical bases for interpreting them, and some of the implications for understanding bulbar function in olfactory perception[32], learning[5] and imprinting[51]. These topics are relevant for electroencephalographic studies of other brain systems and species and for the data accruing from multichannel optical recordings of tissues impregnated with voltage–sensitive optical probes[49]. They will become relevant for spatial analysis of magnetoencephalograms and microelectrode unit activity as technical developments allow use of adequate numbers of channels.

Spatial analysis requires a sufficient number of channels at close enough intervals so that the spatial texture and pattern of activity can be observed in or over a contiguous part of the brain. Description of the receptor field of a single neuron does not qualify, because this does not reveal the spatial activity pattern within the receptor layer or in the nucleus or cortical area to

which the neuron belongs. Likewise, the collection of EEGs from selected scalp placements does not qualify; at best this provides a sample for correlation analysis of activities from different brain structures. Some early examples of spatial analysis are the derivation of phase gradients for the alpha rhythm in humans by Walter[107] in 1953, and the display of spontaneous and click–induced waves in the anesthetized cat by Lilly and Cherry[69] in 1955. Low resolution spatial images of scalp–recorded EEG activity from humans with 16–32 electrodes are now commonplace". Summaries of reports on EEG spatial analysis over the past 3 decades and on the underlying volume conductor theory are in several monographs: Plonsey[89] (Ch. 5), Freeman[25] (Ch. 4). Livanov[70] (Ch. 1), and Nunez[86] (Ch. 7). Other reviews cover the technical procedures of EEG spatial analysis[35] and its implications for philosophy[97] and artificial intelligence[7]. We interpret our results in the language of non–linear dynamics, but our underlying theory is that of axons, dendrites and synapses developed by Sherrington, culminating in his 1929 conception of the central excitatory state[96]. We label our view 'neo–Sherringtonian' in order to emphasize the emergence of our insights from our investigations of the properties of neurons rather than the properties of our mathematical tools.

2. SPATIAL ANALYSIS IN THE OLFACTORY BULB

2. 1. Prior evidence. The rationale for undertaking spatial analysis was to test the hypothesis of Adrian[2] and LeGros Clark[66], that some aspects of olfactory responses to odors might be spatial. The hypothesis was based mainly on the structure of the olfactory system, consisting of a sheet of receptors transmitting in parallel to a cortical sheet of neurons in the bulb, and this in turn to other laminar structures comprising the olfactory cortex. By analogy to other sensory systems the sensory quality of a stimulus was thought to be conveyed by the selection of receptors in an array and intensity by the rates of firing on the selected axons. Preliminary results from microelectrode recording of unit activity in the bulb of the anesthetized hedgehog suggested that neurons responding preferentially to certain odors might be spatially segregated.

Substantial evidence has now accrued from several species showing that single neurons at all levels of the olfactory system including the mucosa [18,55], bulb [60,67,73,75,] piriform cortex [50,84] and orbitofrontal cortex [81,100] respond selectively to presentation of odorants over relatively narrow ranges of concentration with excitation, concentration specific [77] or nonspecific [15]

inhibition, or complex patterns [109] of firing. The specificity of responding is poorly defined, in the sense that each neuron tested tends to respond to multiple odorants [67]. This cross–reactivity holds also at all levels, so that olfactory neurons might be said to be broadly tuned with no evidence for narrower tuning at more central levels. In the terms of Edelman [21] the 'coding' is 'degenerate' as distinct from 'labeled line'. Despite suggestive evidence from genetics and selective anosmias[3] there is no agreement on the numbers of primary odors in olfaction analogous to colors in vision, except that, if they exist at all, and they need not, they might range from[3] 20–30 to as many[66] as 500.

Neurons responding similarly to the same odorant or set of odorants tend not to be homogeneously distributed [79,82,102] in the olfactory mucosa and bulb. Evidence from recording configurations of locally summed receptor slow potentials in the mucosa [72] and of retention times of odorants [83] also indicates that different odorants establish different spatial patterns of activity in the mucosa. The topographic order that exists in the primary olfactory nerve from the mucosa to the bulb [25,66] indicates that spatial pattern differences between odorants should exist in the bulb as well. Prolonged exposure to an odorant has led to selective degeneration of mitral and tufted cells [17], that might reflect induced odor–specific activity patterns.

Regional differences in metabolic activity during prolonged odor exposure have been demonstrated with 2–deoxyglucose in the glomerular laver of the bulb [14,58,64,65,94,98,99]. These latter approaches have not yet had adequate controls done for individual variability; they permit only one odorant for each subject. Nevertheless, the cumulative results lead to the prediction that when two odorants are presented to an animal on randomly interspersed trials, the neural activity induced in the bulb should co–vary between two distinctive spatial patterns that are correlated with the odors. This is not to say that odorant information is 'encoded' in the patterns or that other aspects of the neural activity are unimportant. It is to say that the spatial patterns should exist. and the forms and the conditions in which they are found should be interesting.

Four experiments are described here that were done over the past 12 years. Each yielded some essential insights, that cumulatively led to a coherent picture, although in no case were the results fully consistent with the initial predictions. The conditions in which all of the experiments were done included (a) use of multiple electrodes with simultaneous recordings, (b)

chronic implantation with recording after surgery from animals in aroused or motivated states and (c) observation of spatial patterns in time periods corresponding whenever possible to single inhalations without ensemble averaging. These conditions were based on our expectation that the most interesting patterns would be those found in animals that were in near–normal states of behavior and were responding to the odors in a goal–directed manner.

2.2. *Multiunit recording.* The first experiment[25] was done with ten 40–micron wire electrodes attached to a shaft at intervals of 0.1 mm along a line 1 mm in length. The device was inserted with a miniature stereotaxic drive clamped to a stainless steel well previously mounted surgically and filled with agar over the exposed dorsal bulb. The minimally restrained rabbits were deprived of food 24 h before each recording session and fed immediately thereafter. Odorants were presented in solution with a cotton pledget held before the nose to induce exploratory sniffing, after the electrodes were placed from above into the external plexiform laver (EPL) parallel to the mitral cell layer. Ten preamplifiers, high and low pass filters. threshold detectors, and pulse shapers and 12 oscilloscopes were used to record units and the EEG, along with a pneumograph trace and an EEG trace recorded monopolarly with respect to the nasal bones from a permanent electrode in the bulbar interior. The 22 traces were multiplexed, digitized and stored in core and then on tape.

The results showed that spatially there were marked inhomogeneities in the amounts of unit activity observed in different parts of the bulb. Two regions roughly 2–3 mm across were repeatedly found to have the greatest activity, one in the ventromedial quadrant and the other in the mid–lateral wall of the bulb. No region of the EPL was silent, but minimal activity was found in the dorsal wall. Regular fluctuation with inhalation was the rule; an audiomonitor gave the sound of surf. Activity broadly increased with episodes of behavioral arousal and exploration, and it decreased with apathy and torpor. No relationships were identified between unit activity and odorants.

On the one hand we concluded that the sample from 10 electrodes was far too small to discern the spatial patterns of bulbar activity, and that technical difficulties would preclude adding more channels. On the other hand we observed consistent positive correlations between the amounts of unit activity and the amplitude of the entire spectrum of EEGs (corrected for

depth position with respect to the bulbar dipole) in respect to location in the EPL, respiratory fluctuations and changes in motivated behavior. Statistical analysis demonstrated that the firing probabilities of single cells and the relative frequencies of multiple units oscillated at the same peak frequency as the EEG near the same part of the bulb. From our understanding[25] of the mechanism by which the EEG was generated we concluded that spatial analysis should be done with the EEG prior to further work with units, in order to define sample spaces for unit analysis.

2.3. *EEGs from naive animals.* The second experiment[26].[27] was done with prefabricated arrays of electrodes surgically placed epidurally onto the lateral face of the bulb. Two types were used. One was a set of 64 wires, 0.1 mm in diameter along a line 6.4 mm on the surface. The I–D Fourier transform was done on single measures after linear extrapolation to correct for the digitizing delay (10 /is/read or 0.64 ms/ frame) and on root mean square (rms) amplitudes of EEG segments 100 ms in duration. A cut–off frequency was identified at 1.0 c/mm above which no spectral peaks occurred[26]; this was consistent with the spatial passband of the granule cell field potential generator, that was calculated from a volume conductor model. The other type [19] was an 8 X 8 or 6 X 10 array of 0.25 mm wires with spacings of 0.5 or 0.8 mm that was guaranteed by data from the linear electrode to minimize aliassing. Recordings were made in the behavioral conditions already described; sets of 64 traces were displayed in rasters with a pen plotter.

The outstanding feature of these sets was the commonality over the array of the EEG wave form. The typical pattern of bulbar traces in aroused animals (Fig. 1) was a slow wave closely related to respiration (surface negative with inhalation) and a burst of oscillation in the gamma range (35–90 Hz in the rabbit) on each crest of the respiratory wave. This pattern was common to all channels. Each burst had the same number of peaks and zero crossings. Hence each burst could be described by its peak frequency from the FFT and by 64 X 1 matrices of rms amplitude and of phase with respect to the ensemble average phase calculated by time–lagged correlation. in consideration of the observed spectral peak frequencies the temporal digitizing interval was increased from 1 to 2.5 ms. In further off–line editing only the bursts were saved. These steps reduced the data by nearly 2 orders of magnitude and for the first time provided routine spatial overviews. The 8 X 8 matrices of single frame or rms amplitudes and phases were displayed

by contour plots with second order extrapolation or by density plots, either printed on paper or displayed on an oscilloscope in the form of movies.

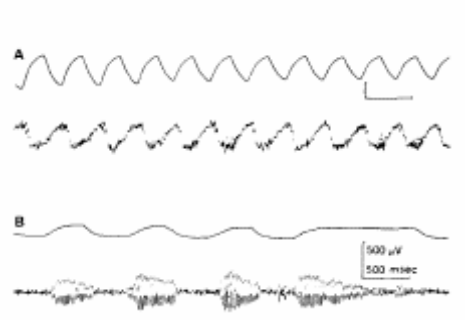

Fig. 1. A: the lower trace shows the EEG from the surface of the olfactory bulb in a hungry rabbit: the upper trace shows respiration measured by a pneumograph. The characteristic EEG pattern is a burst at 60–70 Hz with inhalation (upward) superimposed on a respiratory wave (negative downward)– B: the lower trace shows the EEG from the bulbar surface in a cat under light chloralose anesthesia and with a tracheotomy. The upper trace shows the airflow pulled through the nose (deflection upward) with a respirator attached to the distal end of the trachea. The respiratory wave was filtered from the EEG. The bursts depended on air flow and not on centrifugal input to the bulb from the respiratory centers. because the respiratory rate was about twice that shown for the nasal air flow.

We papered the walls of the laboratory with these plots, discovering that each animal had its characteristic spatial patterns of phase and amplitude, that like signatures were easily recognized but never twice identical [27] (Fig. 2). Bulbar amplitude patterns took the form of foci with half–amplitude diameters averaging about 2 mm, with irregular borders, and with the centers in or presumably just outside of the array. The 8 X 8 arrays were always fixed with the posterior edge at the posterior border of the lateral bulb and the anterior edge over the middle third (see Fig. 8). Thus, the EEG foci were located at a position corresponding approximately to one of two locations of intense activity in the bulb identified by unit recording and the 2–deoxyglucose method. 'these loci. interconnected by associational fibers [92], also corresponded to regions of small glomeruli, small mitral cells and high neural density analogous to retinal foveae[78].

The details of the shapes of foci varied erratically and unpredictably, as did the mean rms amplitude from each burst to the next. The bulbar phase pattern took the form of a gradient averaging 0.25 radians/mm with a range of values roughly ± 0.45 radians over the array, but the orientation of the gradient with respect to the array varied randomly around the clock on

successive bursts. This contrasted with patterns from the prepyriform cortex, which showed multiple peaks of amplitude like islands eccentric to the lateral olfactory tract (LOT) and a phase gradient consistently in the direction of the LOT, that was compatible with its conduction velocity (from 5 down to 2 m/s in these segments)

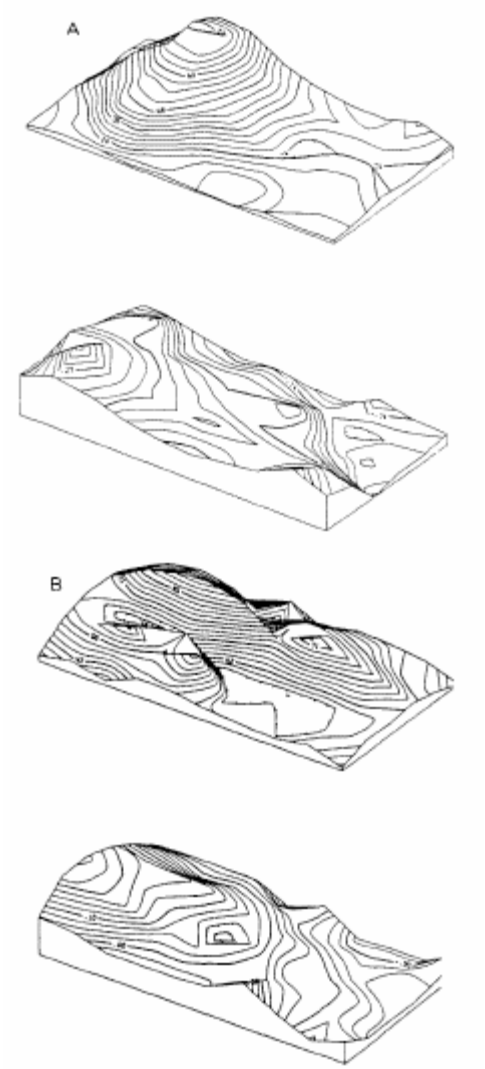

Fig. 2. The upper frames show perspective contour plots in microvolts of the root mean square (rms) amplitude of EEG bursts from 6 X 10 arrays of 60 electrodes at 0.8 mm spacing (4 X 7 mm). The lower frames show the plots of phase in radians with respect to the ensemble average. A: plots from a burst at 59 Hz from a hungry cat with the array on the lateral surface of the bulb; anterior is upward and dorsal is to the right. The amplitude pattern was relatively constant across bursts; the location of the phase maximum or minimum and the direction of the phase gradient varied at random across bursts. B: plots from a burst at 65 Hz from a hungry rabbit with the array on the prepyriform cortex and olfactory nucleus: dorsal is upward and posterior is to the right. The lateral olfactory tract

ran under the middle of the array parallel to the long edge from left to right. The phase gradient was consistent with the 5 m/s conduction velocity of this main segment of the tract and with the 2 m/s velocity of the terminal segments to either side. The maximal amplitudes occurred on both sides of the tract at locations that were relatively stable [27,7] unless the animals were conditioned.

Up to 24 odorants were presented to each animal, and odor bursts were recorded, processed and compared with control bursts. In no instance were consistent differences either in phase or in amplitude found to depend on odorants. The amounts of difference between control and test odor bursts did not exceed the differences between pairs of control bursts, although the animals were commonly observed to sniff to the odorants.

2.4. *EEGs under serial conditioning.* Previous studies of olfactory EEGs repeatedly showed that the major behavioral correlates were between EEG amplitudes and the levels of arousal, motivation and attention[25]. We inferred that detection of an EEG pattern difference with an odorant might require us to train animals to respond to the odorant. Also, we wished to control for possible selective anosmias. In the third experiment[39] we used classical aversive conditioning by pairing each presentation of an odorant as a conditioned stimulus (CS+) with a brief electric shock to the paw or cheek (UCS). The odorant was delivered with a dilution olfactometer [80] and automated solenoid valves into a steady air stream for 3 s, with the UCS given 2.5 s after odor onset. The conditioned response (CR) was measured by the rate of occurrence of sniffing over sets of 10 trials relative to background sniff rate. While not entirely conventional, this autoshaped response had the advantage of becoming clearly established well within 10 trials in a session [16,41], as compared with other CRs such as paw flexion and nictitating membrane retraction that took several sessions to reach criterion. Rapid learning was urgently needed in order to minimize the quantity of EEG data.

In the first session with each of 6 rabbits a difference was found in the spatial pattern of amplitude between the contour plots of the ensemble averages of odor bursts and the control bursts preceding them. These differences did not appear to be statistically significant under Hotelling's T2, linear discriminants, or various types of cluster analysis. An empirical test emphasizing the tails of the distributions was devised, which consisted of computing the 64 t–values for the channel mean differences between 10 control and 10 odor bursts, and calculating a X2 value for the experimental t–distribution against Student's t–distribution. Control–control t–

distributions were found to conform to the latter. The distribution of X2 values was formed for [1180] control–control comparisons from 11,800 pairs of control bursts, and a 97.5% upper limit was defined. Then any control–odor comparison exceeding that limit (e.g. X2 = 100) was inferred to reflect a significant difference for that session, CS+ odorant, and animal (Fig. 3).

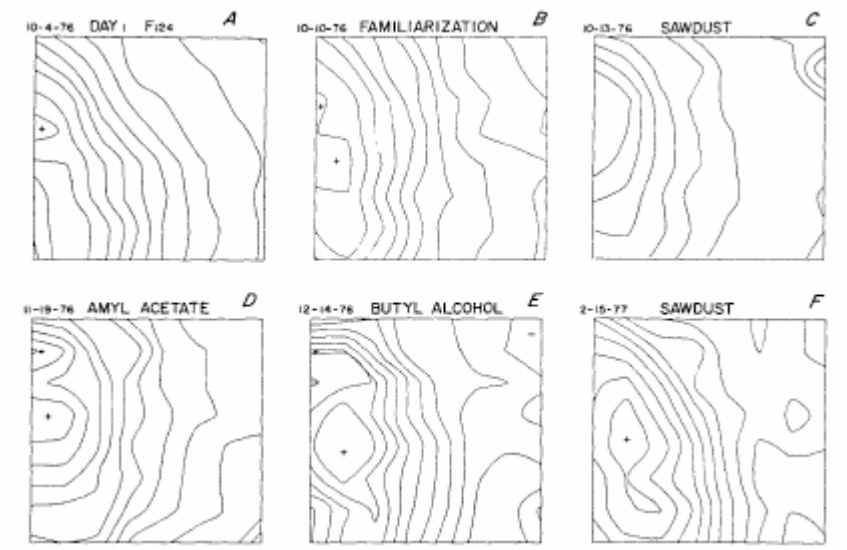

Fig. 3. The contour plots are shown for the mean EEG rms burst amplitude from a trained rabbit over a period of 4 months. In main outline the focus was sufficiently stable to serve as the 'signature' pattern characteristic of this animal. Without conditioning such patterns remained unchanged for months. Under aversive or appetitive conditioning they changed with each new set of stimulus–response contingencies. Examples are shown of 5 such changes with classical aversive conditioning as well as familiarization to the recording apparatus. Presentation in the last stage of the odorant 'sawdust' used in the first stage did not result in return to the EEG Pattern of the first stage [39].

The pattern differences were significant for all animals in the first session, but by the third session they were not. The spatial patterns had evolved to new forms with return to the previous low levels of variance. A new CS+ was presented in the 4th session, and again in the 7th, each time with emergence of a significant difference followed by re–stabilization of a new pattern by the 6th and 9th sessions. Return in the 10th session to the CS+ used in the first session gave another replication with appearance of a new pattern and not the pattern seen with the same CS+ in the first session. The pattern changes did not accompany repeated odorant presentations without reinforcement (CS–) nor presentations of the UCS paired with visual and auditory CS+s.

These results showed that expectancy and its modification by learning played a role in bulbar EEG pattern formation for odor CS+s. They left unanswered the questions how the pattern might differ depending on the presence or absence of the odorant (clearly the animals detected the CS+ odorant, usually in a single inhalation, even though the control and odor bursts did not differ significantly), how an unexpected odorant leading to behavioral responses might affect bulbar patterns, and how expectations of two or more odorants might be reflected in bulbar activity patterns.

2.5. *EEGs under discriminative conditioning*. In the fourth experiment[105] We used classical appetitive conditioning by depriving rabbits of water for 24 h, pairing 1 ml of water with an odor CS+ and not with an odor CS– on randomly interspersed trials, and measuring both the sniff CR– (to the CS–) and the jaw movement CR+ (to the CS+) as a part of the licking response detected electromyographically. The hypotheses were tested that (a) between the times of onset of the sniff signifying detection of an odorant and of the CR+ (if any), odor–specific information existed in the bulb as the basis for decision, (b) that this information would be detectable as a difference in spatiotemporal patterns between bursts with the CS+ and CS– odorants and (c) that both patterns would differ from a pattern C+ and C– characterizing a homogeneous control state preceding the odorants. The test was to measure the bursts and to use the numbers to classify bursts in respect to stimulus condition. A positive outcome would be correct classification of CS+ and CS– bursts above chance levels and not of C+ and C– bursts. Initially, the test was restricted to trials on which correct CR+ and CR– responses had occurred and to the 4 of the 5 subjects that showed significant behavioral evidence for odorant discrimination. The data were taken from the 4th–6th session for development of the measurement and classification procedures.

The matrices of rms amplitudes sufficed to distinguish control from odor bursts but not CS+ from CSbursts. More accurate measurements were made by fitting curves to the 64 traces of each burst. The technique was (a) to form the ensemble time average of the 64 traces, (b) to calculate its spectrum with the FFT, (c) to make initial guesses of the frequency and phase of a cosine from measurements on the peak of the spectrum, (d) to fit the cosine to the ensemble time average using non–linear regression[25,36], (e) to optimize estimates of the amplitude, frequency and phase of a cosine both amplitude– and frequencymodulated linearly over time, (f) to subtract the fitted curve from the data and (g) to repeat the process 4 times. The sum of

these 5 fitted curves incorporated 97% of the variance of the ensemble average. Then (h) the frequency and the modulation parameters were fixed, and the amplitude and phase were determined by regression for each of the 64 traces. This incorporated about 80% of the variance of the bursts. Thereby the 64 EEGs of each burst were decomposed into parts [35,40].

As in a chemical separation procedure, all of the parts (the amplitude and phase matrices, the set of frequency measurements, and the matrices of residuals) were tested in turn for efficacy in classification. The simplest effective test for each set of matrices was to calculate in 64–space a centroid for the C+, C–, CS+ and CS– bursts, to classify as 'correct' each CS+ and CS– burst for which the Euclidean distance from its point in 64–space to its own centroid CS+ or CS– was shorter than to that opposing, similarly to classify the C+ and C– bursts with respect to the C+ and C– centroids, and then to subtract the % 'correct' control bursts from the % 'correct' odor bursts. This percentage difference measure served as a 'touchstone' to locate odor–specific information and to optimize the following 4 procedures for its extraction.

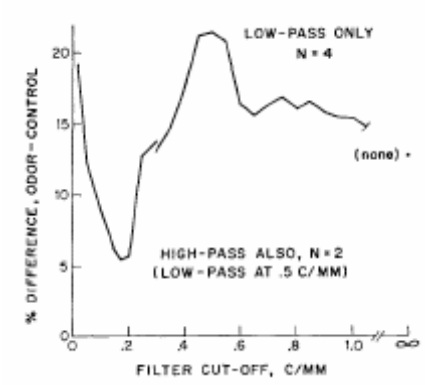

Fig. 4. The ordinate shows the classification efficacy of a Euclidean distance measure (see text) applied to a total of 418 bursts from 4 rabbits trained to discriminate a CS+ from a CS– odorant. It is expressed as the difference between the percentage of odor bursts correctly classified with EEG measurements minus the percentage of control bursts 'correctly' classified (e.g. 76%–55%) on the premiss that control bursts C+ and C– from pre–stimulus intervals were not significantly different. The abscissa shows the cut–off frequency (3 dB fall–off) of a 2–D spatial N–th order exponential filter applied to the amplitude matrices of the dominant EEG components in the spatial frequency domain. The data at the right show that removing high spatial frequencies improved the classification rate with the optimal cut–off frequency between 0.4 and 0.5 c/mm. The data at the right show that the odor–specific information was maximally removed from the EEG with a high pass filter as well set at 0.17 c/mm. This spatial frequency lay in the EEG passband of the granule cells[31,35,37,40]. C/MM, Cycles/mm.

Systematic testing showed that the only fraction containing odor–specific information was the matrix of amplitudes of the largest or dominant component of the bursts, comprising on the average about 50% of the total variance of the 64 EEG traces. Several procedures were found to improve classification efficacy. One was to apply a low pass spatial filter that was designed to conform to the passband of the granule cells and to remove contributions to the EEG from other sources [76]. The filtering was done in the spatial frequency domain[44] by use of the forward and inverse 2–D FFT without Hamming and a 2–D 4th–order exponential filter. Repeated calculation of the touchstone (Fig. 4) over a range of values showed that the optimal cut–off frequency was 0.5 c/mm, and that a minimal touchstone value obtained with a high pass spatial filter set at 0.17 c/mm, thereby attenuating activity at the center of the array passband.

A second procedure was spatial deconvolution [31,35]. The actual spatial activity pattern of granule cells was distorted in its manifestation in the surface EEG in a manner that resembled blurring out of focus of an optical image. The 'point spread function' of the blurring was known from volume conduction studies of the bulb [25,26,34,37,91]. Deconvolution (the ‚software lens') served to re–focus the patterns. Values of the touchstone for a range of focal depths yielded a tuning curve[37,40] with an optimal focal depth at 0.49 mm (Fig. 5), approximately 0.1–0.2 mm above the depth of the mitral cell layer determined post–mortem in these animals.

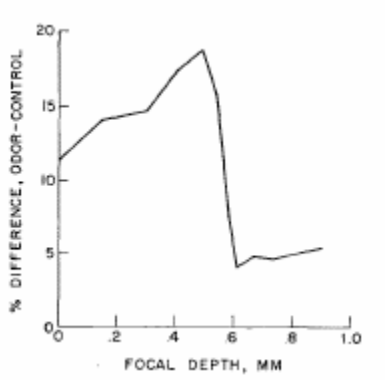

Fig. 5. Spatial deconvolution of the EEG acts as a 'software lens' to compensate for the blurring effect of the volume conductor on the neural activity pattern as it is manifested in the surface EEG pattern. For a dipole field with its zero isopotential surface parallel to the bulbar surface the optimal depth of focus should correspond to the depth of the zero isopotential ('turnover'). In the anesthetized bulb this lay about 0.1 mm above the depth of the mitral cell layer[25,91] (ca. 0.6–0.7 mm in the posterior bulb of the rabbit). The optimal depth of focus by the correct classification criterion was 0.49–0.54 mm. Use of

this procedure requires prior use of low–pass spatial filtering to remove activity from a more superficial dipole in the bulb[76], electrode noise, and possible other contributions to the EEG not from granule cells. The procedure removes the contribution to the EEG from the monopolar reference electrode [31,35,37,40].

A third procedure was channel normalization. Over an entire set of bursts to be classified (e.g. 360 for each animal) the mean and standard deviation (SD) were calculated for each channel, and the data were expressed as z–scores (zero mean and unit SD). This effectively removed the 'signature' pattern of the amplitude focus from the data of each animal and equalized the variances of the contributions of the 64 channels[36].

A 4th procedure, the most effective and important, was prior classification by temporal frequency [35],[36]. The temporal spectrum by the FFT of most bursts had a high, narrow peak between 55 and 75 Hz, but 20% of control bursts and nearly 50% of test bursts had a maximal peak below 55 Hz. These lower frequency bursts tended to have broad spectra with multiple peaks and large frequency modulation in the time domain. Spatially also they were less coherent. Whereas the correlation coefficients of the 64 amplitudes of sets of control, CS+ and CS– odor higher frequency bursts averaged in excess of 0.8, those between lower frequency bursts averaged less than 0.2. Bursts with peak frequencies less than 55 Hz and with FM exceeding 50% of the center frequency were labeled 'disorderly' or 'chaotic'. They did not contain odor–specific information and were deleted (Fig. 6).

2.6. *Analysis of EEG spatial patterns.* Amplitude matrices that were selected and transformed by these procedures were further transformed by factor analysis[35,38,40] into the coordinates of the principal components of the variance. From 4 to 11 factors incorporated 88–96% of the variance. The odor–specific information was converted to factor scores on the factor loadings. Linear discriminant analysis of the factor scores confirmed the validity of the touchstone, and demonstrated 74–100% correct classification of bursts. The analysis was readily extended to trials on which no or incorrect responses had occurred, with lower but still significant ($P < 0.01$ for each animal) classification rates. Each data set served successfully as a 'test' set for cross–classification from the coordinates determined by a 'learning' set. The EEGs from a rabbit that failed behaviorally to discriminate the CS+ and CS– odor in these sessions served to classify correctly odor from control bursts but not CS+ from CS– bursts. Finally, the bursts from each of the 3 sessions irrespective of CR were transformed by factor analysis; each set of factor loadings served to generate factor scores

on the same ('learning') and the other ('test') sets. Classification rates ranged from 58 to 83% correct with no significant differences between test and learning sets. The stability of the factor patterns over the 3 sessions was further demonstrated by cross–correlation of the 3 sets of factor loadings [35,38,40]. Comparable classification results were obtained with alternative statistical procedures [46].

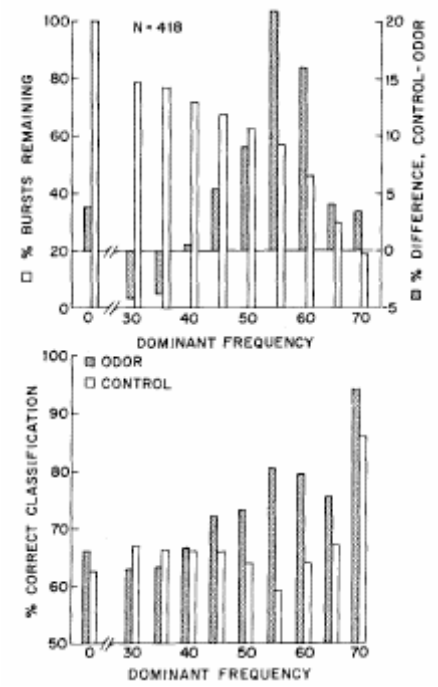

Fig. 6. A finding of major importance was the fact that about 20% of control bursts and 48% of odor bursts do not fall into reproducible categories of spatial amplitude pattern. When they are included in discriminant analysis, they violate the assumption of equal variances among groups and obscure the order that does exist. The key property by which to 'label' these disorderly bursts is their peak frequency in the time domain. The upper graph shows that optimal classification is achieved when bursts with peak frequencies less than 55 Hz are removed before classification. The lower graph shows that when the disorderly bursts are not excluded, or when group sizes become too small, the rate of 'correct' classification of control bursts C+ and C– becomes too high [35,36,40].

The data so far described were taken from 3 sessions out of a total of 18 sessions[105]. Training was in 3 stages of 6 sessions each: odors A+ (reinforced with water) and B– (not reinforced); odors C+ and B–; and odors C+ and A– (reintroduced without reinforcement. The procedures for curve–fitting, filtering, transformation and selection were applied to the data from 5 subjects and all sessions. The classification rates ranged from 58 to 86% correct, averaging 73%, all far above chance levels (33%) for each subject

and session. Cross–correlation of factor loadings revealed factorial invariance within each stage, but sharp breaks between stages at which the S–R contingencies were changed, and at which the factor patterns changed. These breaks corresponded to changes in spatial patterns of rms amplitude that had been shown to occur in the same manner as with spatial pattern evaluation under serial[39] and discriminant[105] conditioning.

These results established the fact that the matrix of amplitudes of the dominant oscillatory component carried odor–specific information. The next question was on which channels. An answer was found by calculating the touchstone value for the sets of bursts from the 4th to 6th sessions of Stage I as before, but deleting 8 channels, then 16, and so forth until only 8 remained. For each number of channels the test was repeated 40 times while a different set of channels was randomly chosen for deletion. After each test an entry was made for each channel used into an 8 x 8 table of the touchstone value resulting. The sum of touchstone values for each channel was divided by the number of times it was used. The channels that were particularly important or unimportant for classification were expected to have mean touchstone values differing from the grand mean over all channels. The entire procedure was repeated on data with and without channel normalization. The results showed that the channel means were normally distributed, and that the average deviation was less than

5% of the grand mean (± 0.5% difference from a grand mean touchstone value of 10.6%). For all animals the classification efficacy decreased steadily with decreasing numbers of channels used (Fig. 7). The results implied that the odor–specific information density was uniform among channels across the array, albeit not necessarily in the bulb at inaccessible spatial frequencies. They terminated 12 years of unsuccessful attempts to correlate features of activity on particular electrodes with the presence of particular odorants.

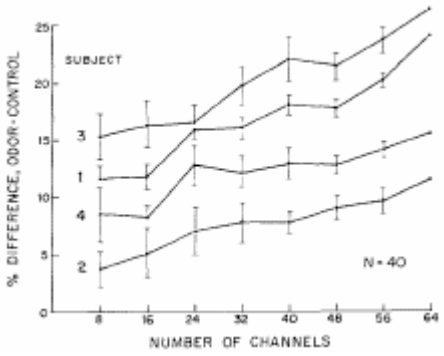

Fig. 7. Channels were selected by a random number generator and their values removed in groups of 8 prior to use of the classification assay. The procedure was repeated 40 times for each rabbit and each number of remaining channels. The means (± S.E.M.) for classification efficacy decreased monotonically with the number of channels remaining. Further testing (see text) showed that the odor–specific information was spatially uniform. The level of the classification assay that was significantly above zero ($P < 0.01$) for each subject was 10.3%; by this criterion two subjects showed significant classification with as few as 8 channels, but only on the average by random selection from the 64 channels.

The 8 X 8 array constituted a window covering about 20% of the bulbar surface area and did not impose a boundary. Concomitant surface and depth recordings 25 from multiple electrodes[9] demonstrated commonality of wave form in the EEG in all parts of the main bulb, whenever it was examined in this regard. The spatial extent of coherence far exceeded the spatial range that could be accounted for by volume conduction alone. Application of the new measurement techniques to the low–amplitude and seemingly random activity between bursts showed that the same commonality held between as well as within bursts; that is, the bulb had a common active state at all times, at least in the waking condition.

Further evidence came from more precise measurements of the bulbar phase gradients (e.g. Fig. 2). On reduction of the error of measurement on single channels in each burst to 0.15 radians (8.5º) it became clear that the gradient was not planar but was conic; that is, the isophase contours formed concentric circles about a point of maximal or minimal phase for each burst. The locations of the extrema were determined by fitting with non–linear regression a cone to the data in spherical coordinates with a radius of 2.5 mm. The fitted surface incorporated on the average 65% of the variance. The conduction velocity of the wave front across the array was estimated for each burst from the ratio of the burst frequency in radians/s (2π times frequency in Hz) to the gradient in radians/mm. The average for the 5 rabbits was 1.73 ± 0.42 m/s. Maxima and minima were about equally likely to occur in both control and odor bursts. The extrema were scattered apparently at random when projected from the sphere onto the bulbar surface (Fig. 8), except that very seldom (< 3% of bursts) were they projected into the posterior quadrant constituting the bulbar stalk. There was no dependence of location or sign of the extrema on stimulus condition[37].

These properties held for both the coherent and the disorderly bursts without significant differences. When the phase values were calculated independently for both the dominant and the secondary components of

coherent bursts and were fitted with cones, the extrema of the two components tended to be located near each other. The signs of the extrema agreed in 95.3% of bursts. The correlation coefficients of the surface coordinates for pairs of extrema averaged 0.79. The mean distance between dominant and secondary extrema was 0.80 mm. Assuming that the two extrema were generated by a common process, that is, that they should have been identical in location, the standard error of measurement was ± 0.28 mm. This was about half the mean interelectrode distance of the arrays. The same results held for disorderly bursts but with slightly greater error ± 0.32 mm).

3. NEURAL DYNAMICS MANIFESTED IN EEGs

3.*1. EEG* oscillations. The salient phenomena to be explained are the oscillations in the gamma range, the bursts with inhalations, the commonality of waveform over the bulb, the formation of reproducible amplitude patterns in respect to odorants, and the non–reproducible patterns between bursts and in disorderly bursts at lower frequencies. The essential mechanism is provided by the mitral (excitatory) and granule (inhibitory) cells that are coupled by dendrodendritic reciprocal synapses[91] into a negative feedback relation.

Demonstration of this relation is afforded by orthodromic or antidromic electrical stimulation of the bulb at low intensity, such that the response amplitude does not greatly exceed that of the ambient EEG[25]. The low–level averaged evoked potential recorded at the bulbar surface closely resembles a damped cosine with an initially negative peak; the field of current is generated by the dendrites of the granule cells and manifests their alternating excitation and inhibition. Post–stimulus time histograms from neurons in the mitral cell layer likewise conform. to a damped cosine at the same frequency and negative decay rate but with a quarter cycle phase lead. On impulse excitation the mitral cells excite the granule cells, are inhibited by them, disexcite the granule cells, and are disinhibited by them. Provided there is a pre–existing level of background activity they are re–excited and another cycle begins. If the stimulus intensity is excessive, the background activity is suppressed and only the first cycle remains as a 'diphasic' evoked potential, easily recorded without averaging. Anesthetics of all kinds also reduce the background activity and thereby truncate the response.

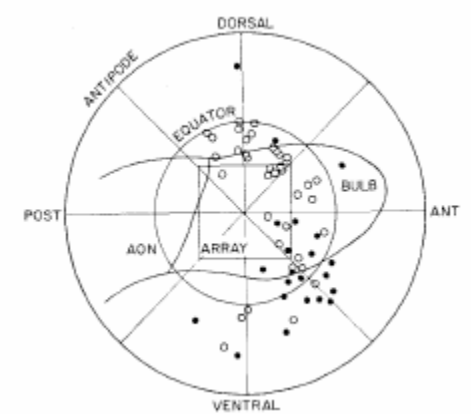

Fig. 8. The left bulb is shown in outline as if viewed from the right side of the head; the rectangle is the outline of the array in its typical location as if seen at its face placed onto the bulb. The rabbit bulb can be approximated as a sphere 2.5 mm in radius. For display purposes the surface of the sphere is presented as a planar surface bounded by a circle at the antipode and centered on the array. The phase pattern of each burst was fitted with a cone in the spherical coordinates so as to capture its pattern of concentric phase contours on the bulbar surface (see Fig. 2A lower part). Distance and angle from the array center to the apex of the cone were used to plot a point in the plane for each burst. It is shown as a solid dot for a phase maximum or as an open dot for a minimum. Both sets of points were randomly scattered over the bulbar surface without regard to odor condition. They were seldom projected into the posterior quadrant where the bulbar surface did not exist[91], those few being regarded as erroneous. The diameter of the open dots is about half the estimated standard error of measurement of the locations of the phase extrema.

Under very deep anesthesia transmission around the loop is blocked. Measurement of evoked potentials in the open loop state gives the open loop time constants of the component neurons. Both the mitral and granule cells have passive membrane time constants averaging about 5 ms. The 4 stages of transmission around the loop for each cycle give a duration of 20 ms and a frequency of 50 Hz. The cycle duration also depends on other factors including the strengths of the synaptic actions that determine the feedback gain, so that oscillation can occur at frequencies in a range from 35 to 90 Hz.

The decay rate of evoked potentials is also determined by several factors, of which the most important is the negative feedback gain. If in a waking animal the stimulus is repeated so as to induce habituation, the response decays more rapidly than at first, implying a more negative decay rate and decreased gain. If the animal is trained to respond behaviorally to the electrical stimulus, the oscillation persists longer, implying that the decay rate is less negative, and the gain is increased. By extrapolation, if factors in attention increase the gain sufficiently, the decay rate may go to zero or

become positive, and a stimulus may evoke an undamped oscillation. This phenomenon cannot be demonstrated with the averaged evoked potential technique, mainly because of the destructive effects of averaging over responses with varying frequency, but the concept can be used to explain the EEG burst with inhalation.

These oscillations are the property of populations of neurons and cannot be explained by entrainment of single neurons [25,57,88,101]. Median firing rate of the bulbar neurons is 10 pulses/s or less, so that each neuron may fire on the average only once in many cycles. Their pulse interval histograms conform to that of a Poisson process with a brief dead time (the refractory period). Their autocorrelograms seldom show oscillation at the EEG frequency owing to the low pulse rates, and their cross–correlograms have vanishingly small shared power. However, statistical averages over relatively long time periods show that the probability of firing of single neurons in the bulb oscillates at the frequency of the bulbar EEG[25].

The demonstration requires digitizing at 1 m/s intervals the EEG from a surface electrode and the pulse train of an underlying mitral cell for 5–15 min, the duration depending inversely on the mean pulse rate (shorter times also with multi–unit recordings). An amplitude histogram (which is almost always nearly normal) is formed of the EEG values in bins arranged in steps of 0. 1 SID from –3 to + 3 SID. A second table for pulses is arranged in two dimensions, one for EEG amplitude and the other for time in 1 ms intervals from –25 to +25 ms. For each EEG value (e.g. 60,000 in 10 min) a unit is entered into the table whenever a pulse occurs within the time bin. The number of pulses in each time bin is divided by the number of occurrences of the EEG amplitude, in order to calculate the pulse probability conditional on time and EEG amplitude. The time average over the 2–D table between +2 and +3 SID of amplitude manifests the pulse probability wave. The ensemble average along the amplitude axis at the times of the upward peaks of the pulse probability wave yields the dependence of pulse probability on EEG amplitude. This experimental relation conforms to a monotonic sigmoid curve that is crucial for EEG analysis (Fig. 9).

3.2. *The static non–linearity underlying bursts.* The bulbar neural mechanism is inherently non–linear. The simplest demonstration is to compare two averaged evoked potentials at different stimulus intensities. Outside of a low–amplitude near–linear range, the larger response to the stronger stimulus has a lower frequency of oscillation. In the population of

coupled neurons there are multiple non–linear transformations around the loop, but each has a near–linear range, and most are kept near–linear by the limitation on activity imposed by the most restrictive or dominant non–linearity. This is found at the trigger zones where dendritic current intensity is transformed to pulse firing rate. Over a narrow range in the resting or background state the pulse rate is proportional to the current amplitude, as measured by the potential difference it causes in passing through the extracellular resistance. With increasing inhibition the neurons are suppressed below threshold, so that pulse rate saturates at zero, and further inhibition is not expressed in the output. Similarly, with increasing activity under excitation, the density of activity of neurons in the population approaches a maximum that is determined not merely by pulse–induced refractory periods but, in the long term, by the time needed for recovery, and by long–lasting post–impulse conductance changes.

The slope of the sigmoid curve, which is the rate of change in axonal output with increment in dendritic input, gives the forward gain of this stage of each population. The product of the forward gains around the loop determines the feedback gain. Close examination of the experimental curves shows that the maximal gain does not occur in the resting state. It is displaced to the excitatory side. This means that an excitatory input to the bulb, such as the receptors deliver during inhalation, not only activates the mitral cells and then the granule cells, it increases their feedback gain. The result is the onset of an oscillatory burst that abates during exhalation. A single shock does not suffice, because the activity it evokes does not last long enough. The requirement is for a surge of axonal input that lasts for tens of milliseconds.

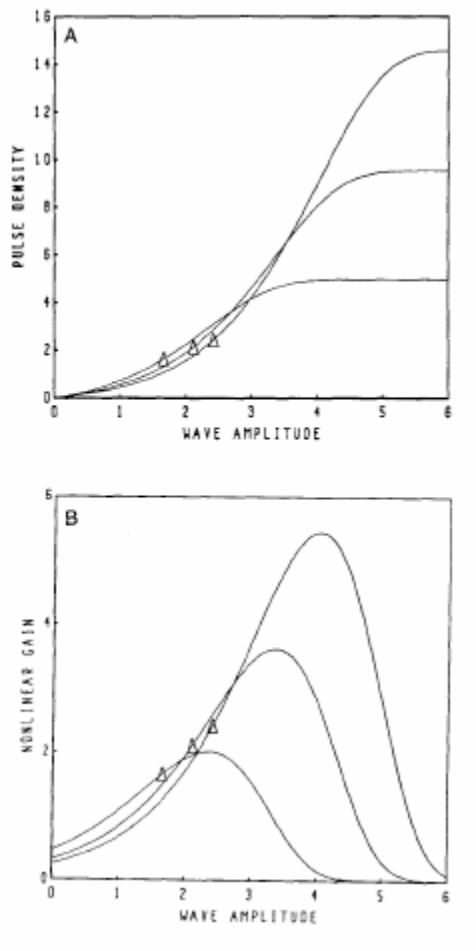

Fig. 9. The static non–linearity of the bulb is determined experimentally from the pulse probability of single mitral cells and small groups conditional on EEG time and amplitude[25], The sigmoid curves in A are derived from a mathematical model that related axonal pulse density in a mass to the intensity of dendritic current[28]. B: the derivative of each curve gives the non–linear gain. The triangles show the mean background values for zero normalized dendritic current amplitude and mean background pulse density. Three examples are shown of increasing an excitatory bias that reflects the level occurring with arousal under centrifugal control. The maximal gain is to the excitatory side of the background level, so that excitatory input from receptors causes a parametric increase in gain in the bulb. This increase underlies the occurrence of the burst.

The experimental sigmoid relation has been closely fitted with a double exponential curve derived from two opposing membrane–dependent processes [28]. On the one hand with increasing membrane depolarization there is an exponential increase in likelihood of firing determined by the voltage–dependent sodium conductance. On the other hand the actual expression of that likelihood in the occurrence of pulses is constrained to a maximal rate that can only be approached asymptotically. Examples of these

curves and their derivatives, the non–linear gains, are shown in Fig. 9. These properties are quite general; we predict that they will be found to hold for neural populations throughout the brain. The shape of the curve holds for all non–zero levels of background activity. Any increase in the background is accompanied by corresponding increases in depolarizing current and in the maximal pulse rate. All 3 variables in the equation for the curves are determined with subsidiary equations from one coefficient that specifies an excitatory operating bias. This bias in the bulb is under centrifugal control by processes relating to arousal or motivation; provisional pharmacological evidence suggests that it is mediated by the centrifugal cholinergic projection to the bulb[93]. The significance of the depolarizing bias for control of negative feedback gain is reflected in the fact that bursts occur in the bulbar EEG only in aroused or motivated animals, and the burst amplitude is directly proportional on the average to the degree of motivation as measured by the duration of food deprivation[25], the rate of work done by animals for food[24], etc.

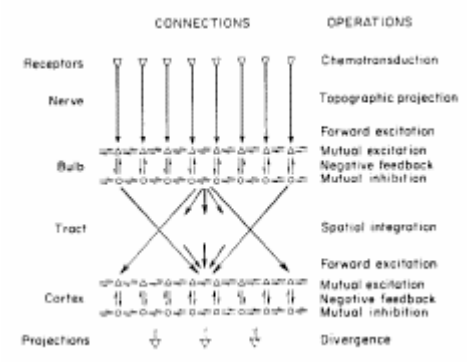

Fig. 10. The first 3 stages of the olfactory system (mucosa, bulb and prepyriform cortex) are shown in outline form, together with phrases to describe the neural operations being done in each stage. The small triangles and circles represent local subsets of respectively excitatory and inhibitory neurons. The arrows represent synaptic transmission[34]. The hypothesis is suggested in Section 4.2 that the prepyriform cortex might function as a motor cortex: that is , the correlates of its neural activity might appear more clearly in respect to responses than to odorant stimuli.

3.3. The commonality of EEG waveform. The neurons in the bulb are arranged in a sheet (Fig. 10) that forms the wall of what Rall and Shepherd[91] have called a 'punctured sphere'. The basal dendrites of the mitral (here including tufted) cells ramify in all directions parallel to the surface for distances in excess of 1 mm from each cell body, forming with their branches a dense feltwork. The dendritic arbors of granule cells thrust through it toward the surface while making bi-directional synaptic contacts

with mitral cells. The input of axons, one each from the [40] million receptors to each bulb in the rabbit, is in parallel to the apical dendrites of the mitral cells. The output is also in parallel by the axons of the roughly 150,000 mitral cells. The input is segregated spatially into encapsulated nests called glomeruli, which form the bulbar equivalent of cortical columns, numbering about 2000 in the rabbit with a mean center–to–center distance of 0.25 mm. The roughly 75 mitral and tufted cells with terminals in each glomerulus and the attendant 30,000 granule cells together comprise a subpopulation that behaves as a neural oscillator. The mitral cells are synaptically coupled with each other by excitatory axosomatic synapses [85] that are also bidirectional[106]. Simulation studies of the stability properties of a model[29],[45] indicate that the granule cells must also interact by mutual inhibition (akin to the network of the eye of Limulus), but the mechanism remains unclear. It is possible that this link is provided by bulbar stellate neurons (the cells of Golgi, Cajal and Blanes), which are equal in size and number to the mitral cells, but about which little else is known. Hence, the bulbar mechanism can be represented by a surface array of non–linear oscillators that are coupled both by mutual excitation and mutual inhibition. So also can the prepyriform cortical mechanism [25].

A dynamic model of the bulb has been embodied in 64 coupled sets of differential equations that incorporate the static non–linearity[30]. The several coefficients in the model that represent time, space and gain parameters have been evaluated physiologically by comparing various numerical solutions of the equations with impulse input to data in the forms of averaged evoked potentials and poststimulus time histograms. For a surge of input patterned after the density of receptor input to the bulb during inhalation the model generates a burst of oscillation having the center frequency in the range characteristic of the EEG and with comparable modulation in amplitude and frequency. Owing to cross–linkages between oscillators in the model all elements share the common wave form, no matter how complex it might appear. This result implies that the synaptic linkages among mitral and putatively among granule cells are likewise responsible for the widespread temporal coherence of macroscopic bulbar activity. Certainly the activity in the gamma range cannot be attributed to synchronized input from receptors, because they lack mechanisms for coordination of their firing at the requisite time intervals, and the variations in conduction velocity and distance of their axons serve to smooth out high frequency fluctuations. Only the low frequency respiratory wave is passed, this being controlled by the brainstem respiratory centers through nasal air flow. Bulbar oscillations clearly persist

after section of the bulbar stalk and even in vitro, so that centrifugal driving cannot explain the commonality. It is a property of the bulb and not of an extrinsic pacemaker[25].

Study of the non–linear dynamics of coupled oscillators is a field still in its infancy, but some general concepts have emerged that are helpful in explaining bulbar dynamics [1,42,53]. A coupled network of realistic numbers (e.g. 64 elements) has an indefinite number of states, but for certain reasonable parameter ranges it displays a manageable number of preferred patterns of activity. Each pattern manifests a dynamic property of the system known as an attractor. Its existence is demonstrated by repeatedly perturbing the system with different inputs and showing that the system returns to one of its preferred states. The domain of input over which this return takes place defines a basin for the attractor.

Three classes of attractors are defined by the character of the preferred activity. If it is rest with steady state or no activity, the attractor is a point reflecting an equilibrium. This occurs for the bulb only under deep anesthesia (the open loop state) or in death. If the activity is periodic, for example, a cosine or any repeating pattern decomposable into a reasonable number of cosines, the attractor is a limit cycle*. The bulb is capable of indefinitely sustained periodic oscillation in certain conditions, such as poisoning by picrotoxin or nicotine, but at abnormally low frequencies. We postulate that bursts manifest the asymptotic convergence to a limit cycle attractor during inhalation, which is aborted during exhalation.

*Mathematicians have pointed out to us that our preliminary estimates [35] on the dimensions of the dynamic processes of the bulbar EEG range between 4 and 6, and that these values are inconsistent with the unit dimension of the 'limit cycle' as strictly defined. One proposed alternative, the low–dimensional attractor', does not serve to distinguish between our 'orderly' and 'disorderly' events. Another alternative, the 'hyper–dimensional toroid' is unsatisfactory because we have no conception at present of the geometry of our putative attractors in phase space. Moreover, the field of non–linear dynamics has not yet adequately developed its own conventions to handle the description of attractors in spatially distributed systems. Further studies will be needed to devise a more rigorous classification than that we use here.

The third type is the chaotic or 'strange' attractor. Its manifestation is activity that appears to be random, but which is deterministic and reproducible if the input and initial conditions can be replicated. Its dimensionality is less than that of random 'noise', although it is difficult to distinguish chaos from an equilibrium that is perturbed by 'noise'[35]. We propose the hypothesis that the

background or interburst activity of the bulb manifests a chaotic attractor in the mechanism. We suggest that the activity arises because the interaction strength of mutual excitation among mitral cells is sufficiently high to sustain regenerative activity; the normalized feedback gain exceeds unity, so that continually their activity tends to blow up. However, they are coupled to inhibitory neurons that dampen their activity and keep it within bounds. A restless and experimentally unpredictable fluctuation emerges at a low amplitude. Most importantly, it is phase–locked over the whole array.

Transition from one attractor to another is called a state change or bifurcation [1,53]. A change in a parameter is required. For the bulb and its model this change is provided by the coupling between input and feedback gain. Whether in the rest state the bulbar dynamics are governed by a point or a chaotic attractor, the input surge and the attendant increase in gain may cause bifurcation to a limit cycle attractor. Order at high amplitude emerges from low–level chaos, only to collapse again as the gain is reduced with exhalation. In this view the bulbar EEG manifests repeated bifurcations at the rate of respiration, with manifestation of recurrent limit cycle states in the bursts. Each state holds for the entire main bulb for the duration of the bursts on the order of 50–150 ms or more.

3.4. Odor–specific information in the EEGs. The information that serves to classify bursts correctly with respect to stimulus condition is uniformly distributed among the amplitude coefficients of the dominant component of the coherent, higher–frequency bursts. This implies that in the presence of a certain odor complex, which most commonly is the background or control complex but may be an odorant CS, upon bifurcation the oscillation tends to converge to a definite and reproducible spatial pattern of amplitude modulation. The details of the phase, the center frequency, and the temporal amplitude and frequency modulation are insignificant. The existence of each stable pattern depends on a successful learning process that results in emergence of discriminatory behavior. We infer that for each discriminated odorant a learned limit cycle attractor forms, which is distinguished from others in its class by its basin, mediated by the receptors that were activated during training, and by its spatial amplitude pattern.

A mechanism of synaptic change that we propose to explain these findings is based on earlier studies of the change in the shape of averaged evoked potentials from the prepyriform cortex of cats as they were trained to press a bar for milk in response to electrical stimulation of the lateral olfactory tract

[23,25]. The same coordinated and sustained pattern of change in waveform was found in the bulb on appetitive conditioning of rats to LOT stimulation and in the superior colliculus on appetitive conditioning of cats to optic tract stimulation (unpublished data). The change consisted in a decrease in phase, frequency and decay rate, of the dominant damped cosine fitted to the responses.

Simulation of this pattern change with the solutions to piece–wise linear and non–linear differential equations modelling the dynamics of bulb or cortex [29,35] demonstrates that the only change in the equations that suffices to replicate the change in response waveform is a small increase in the coefficients representing the strength of synapses from excitatory neurons onto other excitatory neurons, that is, by an increase in mutually excitatory feedback gain among elements representing local subsets of excitatory neurons. A modest increase of 40% can increase the sensitivity of a local oscillator 40,000 fold. This is because of the combination of excitatory positive feedback with the amplitude–dependent non–linear gain; small inputs can explode into large outputs providing that they last long enough. The coupling with negative feedback ensures that the output is oscillatory and not monotonic, and that the oscillation terminates after cessation of input.

When the mutually excitatory connections in the model are strengthened among a subset of elements, for example 8–16 out of an array of 64 oscillators, input to any one or more activates the others preferentially, so that the spatial pattern of output reflects stereotypically the template of the strengthened connections and not the locus of the input. This system closely resembles the nerve cell assembly of Hebb[52,104]. We conceive that on each inhalation during conditioning an odorant activates multiple receptors within a subclass that is sensitive, and these in turn co–activate a subset of mitral cells. If reinforcement is given, then the bi–directional synapses that couple the concomitantly active neurons are strengthened. Over several trials with 10–20 inhalations on each trial, a large fraction of the subclass of sensitive receptors is stimulated by random selection owing to turbulence in nasal airflow, and the nerve cell assembly is enlarged by pair–wise co–activation of the mitral cells to which they project. Thereafter any input to small numbers of receptors in that fraction activates the entire assembly preferentially.

Recent evidence indicates that reinforcement is mediated in the bulb by norepinephrine presumably under control of the locus coeruleus. Injection of the beta–blocker propanolol into the bulb blocks the EEG pattern changes that otherwise occur on presentation of odorants with shock, whereas intrabulbar infusion of norepinephrine enables pattern changes to odorants without reinforcement, that otherwise do not occur [47].

In the model and by inference in the bulb, if bifurcation does not occur, the stimulus–evoked activity remains localized to the nerve cell assembly, but with onset of the limit cycle oscillation of the burst, the entire system engages in activity. The stereotypic output pattern is global, both in the sense that it involves all elements and that each local region, such as the fraction of the bulb covered by the array, contains all of the information at reduced resolution compared with the whole. In this respect though not in others bulbar output may resemble a holographic storage pattern.

The significance of the phase extremum for each burst is that it may occur at the site of nucleation, that is, the spatial location at which the bifurcation from chaos to a limit cycle begins. The phase extrema from successive bursts vary at random over the bulbar surface both in location and in sign. The extrema for the dominant and secondary frequency components of individual bursts tend to conform closely in sign (phase lead or lag) and in location; the conduction velocities, both measured over a part of the bulb flattened by the array, also closely agree. The velocity of apparent propagation, 1.73 m/s, may depend on the conduction velocity of the axon collaterals of mitral cells; the velocity of mitral axon terminal segments in the prepyriform cortex (Fig. 2) is 2 m/s 25. From the size of the rabbit bulb (1.5 mm in radius at the depth of the collaterals) and the typical frequency of oscillation (60–70 Hz) the bifurcation is completed in about 1/6 cycle (2.5 ms). The same should hold for the larger bulb of the cat with frequencies of 35–45 Hz10 and the smaller bulb of the mouse with frequencies of 75–90 Hz20. In these few milliseconds the likelihood of formation of two or more competing sites of nucleation would seem to be small; evidence for it was sought in the form of disparate phase extrema between the dominant and secondary components of orderly and disorderly bursts, but none was found[37].

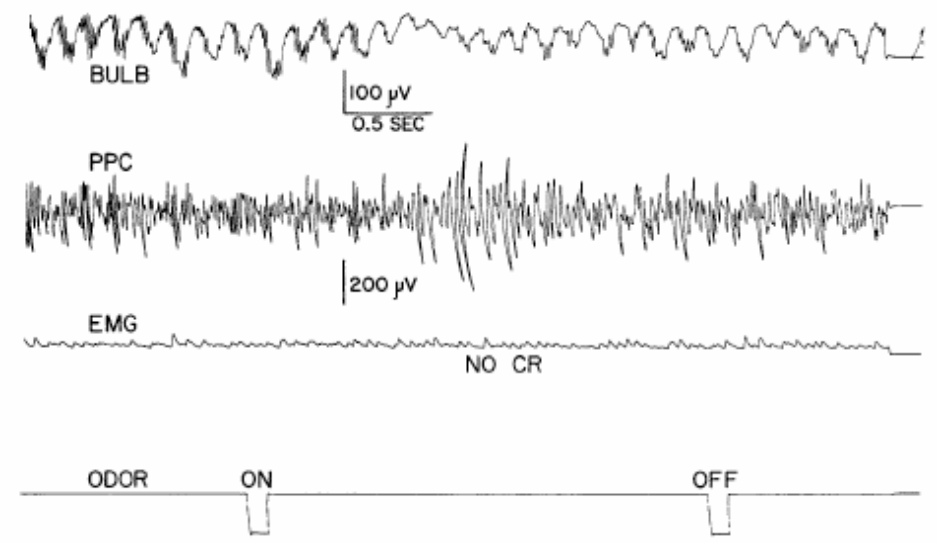

Fig. 11. An example is shown of high–frequency burst suppression in the bulbar EEG by presentation to a rabbit of a novel odorant, which elicited a sniffing response but not a conditioned response (paw flexion) as did an odorant CS+. The EEG of the prepyriform cortex (PPC) showed an episode of erratic low frequency activity that we suggest may reflect chaotic as distinct from 'noisy' activity in the bulb and the prepyriform cortex to which it transmits. Evoked potential studies[25] suggest that the cortex acts as a resonating receiver with broad response bands in two or more frequency ranges.

3.5. *The disorderly bursts: chaos?*

Close to 20% of control bursts and 50% of odor bursts of both kinds have broad temporal spectra with multiple peaks, and the largest peak is typically at a frequency between 20 and 40 Hz. The modulation of the center peak frequency commonly exceeds 50% over the recorded duration of the burst (76 ms). The spatial amplitude patterns of the 5 cosine components do not serve to classify bursts and do not fall into reproducible categories. An explanation of these bursts is that they manifest failure of the bulbar mechanism to converge to a limit cycle attractor but possibly to a chaotic attractor.

This type of activity also occurs when rabbits are presented with a novel odor in relatively strong concentration (Fig. 11). Regular bursts of the control state are replaced by low amplitude aperiodic activity having a broad spectrum with its largest peak below 55 Hz. The frequency shift distinguishes it from interburst activity. Our interpretation is that a limit cycle attractor does not exist to serve as a focus for convergence. Almost invariably rabbits orient to the stimulus for several trials; thereafter, both the EEG change and the orienting response abate and disappear, if the odorant is not reinforced. This suggests that the disorderly burst in itself may mediate the orienting response. A possible mechanism is that the prepyriform cortex operates as a tuned filter to which the bulb transmits

its oscillatory output. Spectral analysis of the impulse responses reveals multiple resonant peaks, particularly those in the normal transmission range above 55 Hz, but also in the range of 20–40 Hz. Therefore, the disorderly burst may serve first as a signal that convergence to a limit cycle attractor has failed, and thereafter by repetition that an unknown odorant is present, constituting a departure from the status quo. The persistence of the status quo is signaled by the control bursts.

3.6. Limitations of the approach. The first difficulties in spatial analysis were those of hardware in getting enough simultaneous measurements to enable the assembly of spatial images. Thereafter the problems lay in developing the software needed to manage masses of data and extract the significant features. The solutions described here were to use spatial and temporal spectral analysis to determine optimal sampling rates, digital filters to decompose the data into space–time components and residuals, and a behaviorally based assay to evaluate event–related information in the several fractions. The results led to the problem of interpretation; our approach was to embody the known anatomy, physiology and pharmacology of the bulb in a set of differential equations, solve the equations for input, initial and boundary conditions simulating those holding in normal behavior, and compare the solutions of the equations expressed as curves with the results of measurement expressed as data points. When they conformed we transferred our explanation of the dynamics from the model to the bulb, using the languages of neurobiology and non–linear dynamics. The over–riding problem was to maintain the brain in a normal functional state. We solved this by adapting our recording systems for use with permanently placed electrodes in animals subjected to conditioning procedures.

Present problems exist at all levels. One is getting enough sensors on or into the brain for long–enough periods to allow behavioral studies without damaging the brain or impairing the health of the animal. The present limit to 64 channels is imposed more by the size of the connector cemented to the skull than by the availability of amplifiers, multiplexers, and core to handle the data flow. Another is the restriction to recording from laminar structures, particularly the lissencephalic cortices found in simpler mammals. Management of the difficulties of sampling and *3–D* analysis of data from nuclei and folded laminar structures such as the hippocampus seems beyond feasibility at present. So also is the management of data from *64* or more micro–electrodes, although the use of optical sensors seems promising as a source of data on unit activity [49].

The field potentials such as the EEG suffer from the smoothing effect of the volume conductor especially for scalp electrodes but also for cortical electrodes on and under the surface. In the bulb the attenuation with spatial frequency is 10–fold with each increment of 0.5 c/mm, at the spatial frequency of the glomeruli, which are likely to determine the 'grain' of bulbar macroscopic activity patterns, the attenuation is 10–4, so that the detail of bulbar activity patterns is irretrievably lost from the EEG even with closely spaced electrodes. Surgical access to many parts of the brain is limited either by circulatory vessels, afferent pathways or gyrification. These shortcomings, are to some extent offset by the robustness of the macroscopic activity. High classification rates of bulbar EEG bursts were found despite restriction of the spatial sample to 115 of one bulb, at a spatial sampling frequency 1/4 of the optimal, over a time base 1/10 that available to the animals, and on signals that were often not much above the amplifier and electrode noise levels. In fact the system did slightly better in EEG discrimination than did the animals in responding correctly to odorants [38,105].

Limitations also restrict our use of non–linear dynamics to selected simulations of representative events with solutions of the equations by numerical integration. This is less than adequate for constructing representations of the phase space of the model[7]; even could we do this the available algorithms for graphic display might be insufficient. A large part of work being done in non–linear dynamics is devoted to exploring the complex behavior that can be elicited from standard 'simpler systems' such as coupled Van der Pol oscillators, the inverse problem of constructing a model given the behavior cannot be generalized. The bases for model–building in neurophysiology are too far removed from those of hydrodynamics, plasma physics, theoretical chemistry, embryology, etc., for more than the exchange of analogs and anecdotes. Diffusion, for example, is replaced by axonal conduction. The dimensions and characteristic exponents of putative EEG limit cycle and chaotic attractors are still under initial study[6,35]. From the perspective of neurobiologists the bulb is a 'simpler system', but the dynamics of 2000 coupled non–linear oscillators with indefinite numbers of chaotic and limit cycle attractors, continually perturbed by ‚noise' and changing state 5–10 times per second, is not so regarded by mathematicians.

Our ability to distinguish chaos from equilibrium under perturbation is inadequate[35]. The fractal dimensions and Lyapunov exponents have not been measured reliably. Chaos is likely to play major roles, first in the

background state as the means for giving rapid access to any of a collection of limit cycle attractors on each inhalation, second as a means for expressing failure of convergence, and third as a vehicle for information of kinds not yet defined. This area of EEG studies will be of major importance in the next decade.

4. IMPLICATIONS FOR NEUROPHYSIOLOGY

4. 1. Sensory systems and perception. Despite the complexity of its details, spatial analysis offers a simple and compelling answer to the question of how the diverse synaptic input to sensory cortex from multiple and often widely separated axons within the duration of a sniff or a saccadic interval is integrated with past experience into a percept. Our answer is that the input initiates (a) a local spatial pattern of activity that is shaped by a pre–existing nerve cell assembly, and (b) a parametric increase in gain that causes a state change from pre–existing low–level chaos to a high–level limit cycle carrier. The amplitude modulation pattern is selected by the input and shaped by the assembly; each local part of the bulb takes an amplitude of oscillation that is determined by the whole. Each local region transmits the whole with a degree of resolution determined by its size relative to the size of the bulb. Thus the input is local and after the bifurcation the output is global.

The data show that this happens in olfaction; the spatial analysis shows the manner in which it can take place. The next question is whether this transformation occurs in other sensory systems as well. The likelihood that it does is enhanced by several similarities among sensory systems in structure and function. All contain arrays of receptors that feed in parallel to arrays of neurons, usually through relays but always ultimately to laminated neuropil in cortex. The cortex contains large numbers of densely interconnected excitatory and inhibitory neurons with the requisite 3 kinds of synaptic feedback. Again the output of cortex is in parallel by large numbers of axons. Although the bulb has many specialized anatomical and physiological traits peculiar to it, the only properties needed for the simulation of its key operations are those that it has in common with other systems: parallel input and output and synaptically coupled masses of excitatory and inhibitory neurons with the voltage–dependent membrane conductance of the action potential.